Journal of Neurochemistry

JOURNAL OF NEUROCHEMISTRY | 2016 | 136 | 1219–1231 doi: 10.1111/jnc.13506

ORIGINAL ARTICLE

Dopamine induces mitochondrial depolarization without activating PINK1-mediated mitophagy

Heather Bondi,*,† Mara Zilocchi,*,† Maria Gabriella Mare,* Gianluca D'Agostino,*,‡ Stefano Giovannardi,* Santiago Ambrosio,‡ Mauro Fasano*,† and Tiziana Alberio*,†

*Division of Biomedical Research, Department of Theoretical and Applied Sciences, University of Insubria, Busto Arsizio, Italy

†Center of Neuroscience, University of Insubria, Busto Arsizio, Italy

‡Biochemistry Unit, Second Department of Physiological Sciences, University of Barcelona, Barcelona, Spain

Abstract

Parkinson's disease (PD) is one of the most prevalent neurodegenerative disorders, characterized by the loss of dopaminergic neurons in the substantia nigra pars compacta. PD mostly occurs sporadically and its cause remains unknown, nevertheless the discovery of familiar forms of PD, characterized by mutations of genes encoding proteins associated with mitochondria homeostasis, suggests a strong implication of the mitochondrial quality control system in PD. We investigated the effect of dopamine cytosolic accumulation in undifferentiated SH-SY5Y cells, an *in vitro* model widely used to reproduce impairment of dopamine homeostasis, an early step in PD pathogenesis. A strong depolarization of the mitochondrial membrane was observed after dopamine exposure. Nevertheless, mitochondrial network resulted to assume a peculiar morphology with a distinct pattern of OPA1 and MFN1, key regulators of mitochondrial dynamics. Moreover, selective elimination of dysfunctional mitochondria did not take place, suggesting an impairment of the mitophagic machinery induced by dopamine. Indeed, PINK1 did not accumulate on the outer mitochondrial membrane, nor was parkin recruited to depolarized mitochondria. Altogether, our results indicate that an improper handling of dysfunctional mitochondria may be a leading event in PD pathogenesis.

Keywords: dopamine, mitochondria, mitophagy, parkin, Parkinson's disease, PINK1.

J. Neurochem. (2016) **136**, 1219–1231.

Impaired dopamine homeostasis is a common trait in Parkinson's disease (PD) pathogenesis (Lotharius and Brundin 2002; Caudle *et al.* 2008; Alberio *et al.* 2012). Leakage of dopamine from pre-synaptic vesicles (e.g., due to α-synuclein oligomers) is at the basis of oxidative stress conditions, the impairment of mitochondrial functionality and the consequent susceptibility of nigral dopaminergic neurons (Lotharius and Brundin 2002; Hauser and Hastings 2013). When stored in vesicles, dopamine spontaneous oxidation is prevented by the acidic environment, whereas cytosolic dopamine rapidly gives rise to semiquinonic and quinonic species with the concurrent production of reactive oxygen species (ROS) (Lotharius and Brundin 2002; Guillot and Miller 2009).

Mitochondria are major intracellular sources of ROS, produced as byproducts of ATP synthesis through the electron transport chain. A vicious cycle of oxidative stress

Received September 11, 2015; revised manuscript received November 19, 2015; accepted December 8, 2015.

Address correspondence and reprint requests to Tiziana Alberio, Division of Biomedical Research, Department of Theoretical and Applied Sciences, University of Insubria, via Luciano Manara 7, I-21052 Busto Arsizio, Italy. E-mail: tiziana.alberio@uninsubria.it

Abbreviations used: BSA, bovine serum albumin; CCCP, carbonyl cyanide m-chlorophenylhydrazone; COX5B, cytochrome c oxidase subunit 5B; DAPI, 4′,6-diamidino-2-phenylindole; DMEM, Dulbecco's modified Eagle's medium; DMSO, dimethylsulfoxide; ECACC, European collection of cell cultures; FBS, fetal bovine serum; fov, field of view; IMM, inner mitochondrial membrane; MFN1, mitofusin 1; MTS, mitochondrial targeting sequence; OMA1, overlapping with the m-AAA protease homolog; OMM, outer mitochondrial membrane; OPA1, optic atrophy 1; PBS, phosphate-buffered saline; PD, Parkinson's disease; PINK1, PTEN-induced putative N-terminal kinase 1; PVDF, polyvinylidenedifluoride; RIPA, radioimmunoprecipitation assay; ROS, reactive oxygen species; SDS, sodium dodecyl sulfate; TBS-T, Tris-buffered saline with Tween 20; VDACs, voltage-dependent anionic channels.

and mitochondrial damage can spread rapidly into the intact mitochondria (Alberio *et al.* 2012; Hauser and Hastings 2013). In addition, DA-quinones induce a direct modification of protein subunits of complex I and complex III of the electron transport chain, leading to an impairment of mitochondrial respiration and to an increase in ROS production (Van Laar *et al.* 2009).

Several quality control mechanisms must preserve mitochondrial homeostasis and prevent cellular damage. Mitochondrial dynamics, fission and fusion processes, which regulate the extension and morphology of the mitochondrial network, play a crucial role in the mitochondrial quality control (Youle and van der Bliek 2012). Both processes are highly regulated in response to various physiological cues (Franco-Iborra *et al.* 2015). Severe mitochondrial damage and membrane depolarization suppress fusion, leading to fragmentation of the mitochondrial network. Fusion suppression in damaged mitochondria is mostly led by the Overlapping with the m-AAA protease homolog (OMA1), which inhibits inner mitochondrial membrane (IMM) fusion by cleaving optic atrophy 1 (OPA1) and by selective degradation of mitofusins essential for outer mitochondrial membrane (OMM) fusion (Kornmann 2014). Consequently, damaged mitochondria are selectively removed through an autophagic process called mitophagy, where entire mitochondria are engulfed in double-membrane vesicles, known as autophagosomes, and are delivered to lysosomes for degradation (Narendra and Youle 2011).

The most well-recognized mechanism governing the recruitment of autophagosomes to mitochondria is that driven by the PTEN-induced putative N-terminal kinase 1 (PINK1)/parkin pathway (Narendra and Youle 2011). Under physiological conditions, PINK1 rapidly translocates the intermembrane space and is processed to a shorter form that undergoes proteolytic degradation. Following mitochondrial depolarization, PINK1 is no longer degraded by mitochondrial proteases; rather, it is exposed on the OMM of depolarized mitochondria in its full-length form (Jin *et al.* 2010; Jin and Youle 2012), recruits parkin (an ubiquitin-E3-ligase that ubiquitinates OMM integral proteins, such as VDACs – voltage-dependent anionic channels – and mitofusins), and triggers mitophagy (Narendra *et al.* 2010; Jin and Youle 2012). Noticeably, PINK1 and parkin were associated to autosomal-recessive parkinsonisms (Bonifati 2012). Impaired mitochondrial quality control results in the accumulation of damaged mitochondria that may generate higher levels of ROS, produce ATP less efficiently and have a lower threshold for cytochrome c release and apoptosis activation (Pickrell and Youle 2015).

Although mutations in PINK1 and parkin are linked to familiar forms of PD, sporadic PD might be the result of other concurrent mechanisms that eventually converge on the impairment of mitochondrial function (Alberio *et al.* 2012). In accordance with this view, we explored the alteration of the mitochondrial network, mitochondrial dynamics and mitophagy because of dopamine-induced toxicity, using the undifferentiated SH-SY5Y human neuroblastoma cell line. In these cells, it is possible to mimic the improper handling of the dopamine neurotransmitter thought to occur in dopaminergic neurons of PD patients, as their ability to take up dopamine via the dopamine transporter is higher than their capability to store it into vesicles (Mena *et al.* 1989). Thus, it is possible to reproduce this leading event in PD pathogenesis by the administration of exogenous dopamine in the culture medium (Alberio *et al.* 2010a,b; Alberio *et al.* 2012, 2014a,b; Gomez-Santos *et al.*, 2003). Eventually, this cell line is widely used to investigate mitochondrial dynamics in PD (Gegg *et al.* 2010; Geisler *et al.* 2010; Matsuda *et al.* 2010).

Methods

Cell culture

Human neuroblastoma SH-SY5Y cell line was obtained from the European collection of cell cultures (ECACC, Cat No. 94030304; Lot No. 11C016). Cells were maintained at 37°C under humidified conditions and 5% CO_2 and were grown in High Glucose Dulbecco's modified Eagle's medium (DMEM) supplemented with 10% fetal bovine serum (FBS), 100 U/mL penicillin, 100 μg/mL streptomycin, and 2 mM L-glutamine. All cell culture media and other reagents were from Euroclone.

Cell treatments and subcellular fractionation

Cells were seeded at a density of 1.4×10^7 cells per flask in T225 flasks 24 h before treatments. For dopamine treatments, cells were exposed to 250 μM dopamine in the presence of 700 U/mL catalase to eliminate unspecific effects because of dopamine auto-oxidation (Blum *et al.* 2000) for 6 and 24 h, whereas, for carbonyl cyanide m-chlorophenylhydrazone (CCCP) treatments, cells were incubated in medium containing 20 μM CCCP or an equal volume of vehicle (dimethyl sulfoxide, DMSO). For co-treatment with both dopamine and CCCP, cells were exposed to 250 μM dopamine in the presence of 700 U/mL catalase and 20 μM CCCP for 24 h. Dopamine treatment concentration and time of exposure have been set in previous works (Alberio *et al.* 2010a, 2012, 2014a,b). The CCCP concentration was chosen according to the literature (Geisler *et al.* 2010; Narendra *et al.* 2010; Gao *et al.* 2015). Cells were detached with trypsin-EDTA, collected by centrifugation (300 *g*, 4°C, 7 min) and washed with ice-cold phosphate-buffered saline (PBS). Part of the cellular suspension was kept for whole-cell analysis, whereas the remaining sample was centrifuged again and used to obtain mitochondrial enriched fractions by differential centrifugation protocol, as previously described (Frezza *et al.* 2007; Alberio *et al.* 2014b).

Quantitative western blot analysis

Proteins were extracted using radioimmunoprecipitation assay (RIPA) buffer containing 0.1% sodium dodecyl sulfate (SDS) (50 mM Tris-HCl pH 7.6, 150 mM NaCl, 1% sodium deoxycholate, 1% NP-40 and 0.1% SDS). Cells or subcellular-enriched

pellets were lysed in the appropriate amount of buffer and incubated on ice for 30 min. After that, the lysates were centrifuged at 15000 *g* for 40 min at 4°C, and the supernatant was collected. Equal amounts of protein (80 μg for whole-cell lysates or 40 μg for mitochondria-enriched fractions) were incubated in Laemmli loading buffer, resolved in 10% or 13% SDS-gels and transferred to polyvinylidenedifluoride (PVDF) membranes (Millipore Corporation, Bedford, MA, USA) at 1.0 mA/cm^2, 1.5 h (TE77pwr; Hoefer, Holliston, MA, USA). PVDF membranes were saturated in Tris-buffered saline with 0.05% Tween 20 (TBS-T) containing 5% dried skimmed milk or 5% bovine serum albumin (Sigma-Aldrich, St. Louis, MO, USA). Blots were probed with antibodies against OPA1 (HPA036927, 1 : 250; Sigma-Aldrich), mitofusin 1 (MFN1, sc-50330, 1 : 1000; Santa Cruz Biotechnology, Santa Cruz, CA, USA), PINK1 (#6946, 1 : 1000; Cell Signaling Technology, Beverly, MA, USA) in 5% bovine serum albumin-TBS-T, cytochrome c oxidase subunit 5B (COX5B, #C4498, 1 : 1000; Sigma-Aldrich) in 5% milk-TBS-T, or β-actin (GTX23280, 1 : 3000; GeneTex, Irvine, CA, USA) in 5% milk-TBS-T. Blots were incubated with proper peroxidase-conjugated secondary antibodies, i.e., anti-rabbit (#AP132P, 1 : 1500; Millipore Corporation) and anti-mouse (#12-349, 1 : 3000; Millipore Corporation) in 5% milk-TBS-T. Peroxidase signals were visualized by chemiluminescence using enhanced chemiluminescence substrate (Millipore Corporation). Images (16 bit grayscale) were acquired with G:BOXChemi XT4 (Syngene, Cambridge, UK) system and analyzed using ImageJ software (National Institute of Health, Bethesda, MD, USA). β-Actin and COX5B contents were established as loading controls for whole-cell and mitochondrial loading controls, respectively. All experiments were run in at least three replicates for each condition.

Measurement of mitochondrial membrane potential ($\Delta\Psi_m$)

SH-SY5Y cells were seeded in 24-well plates at 1×10^5 cells per well and cultured for 24 h at 37°C before treatments. Cells were treated with 250 μM dopamine in the presence of 700 U/mL catalase for 6 and 24 h. As a positive control for mitochondrial depolarization, cells were treated with 20 μM CCCP (from a 2 mM stock solution in DMSO) for 24 h and compared to cells treated with the same DMSO concentration (Matsuda *et al.* 2010). To evaluate the mitochondrial membrane potential at the end of each treatment, media were removed and replaced with fresh DMEM with 100 nM Mitotracker Red CMXRos (chloromethyl-X-rosamine; Life Technologies, Grand Island, NY, USA), which accumulates in the matrix of mitochondria with intact mitochondrial membrane potential. After 20 min of incubation at 37°C, media containing Mitotracker were replaced with fresh PBS and cells were fixed with 4% paraformaldehyde for 15 min. Nuclei were stained with 300 nM 4′,6-diamidino-2-phenylindole (DAPI) for 3 min (Life Technologies).

Images were acquired through a cooled CCD camera (Sensicam; PCO, Kelheim, Germany) and a 40× objective on an Olympus IX81 microscope (Olympus, Tokyo, Japan), equipped with variable light attenuation (Lumen 200; Prior Scientific, Rockland, MA, USA) and analyzed using ImageJ software. For each whole field of view (fov), Mitotracker signal intensities were calculated measuring integrated density values (the total intensity of fluorescence in the defined area) minus the mean of background fluorescence values. The corrected intensity was normalized as previously reported (Alberio *et al.* 2014a) with respect to the number of cells, as defined by nuclear staining with DAPI. At least four fovs obtained from three independent experiments were evaluated for each condition. Data are represented as mean ± SEM. Statistical analysis was performed with the Student's paired *t*-test with Welch correction for heteroscedasticity.

Immunofluorescence stain

SH-SY5Y were seeded onto 18 mm glass coverslips in 12-well plates at 7×10^4 cells per well and were allowed to adhere under routine culturing condition for 24 h. Cells were treated with 250 μM dopamine in the presence of 700 U/mL catalase, otherwise with 20 μM CCCP or an equal volume of vehicle (DMSO) for 24 h. Cells were washed with PBS and fixed with paraformaldehyde (4% w/v) for 15 min, permeabilized with Triton X-100 solution (Triton X-100 0.2% in PBS) for 5 min and blocked with 5% FBS in PBS for 1 h. Coverslips were incubated with primary antibody against PINK1 (sc-32584, 1 : 200; Santa Cruz Biotechnology), parkin (sc-32282, 1 : 20; Santa Cruz Biotechnology), COX5B (C4498, 1 : 200; Sigma-Aldrich) and β-tubulin (T4026, 1 : 200; Sigma-Aldrich) in 5% FBS in PBS, overnight at 4°C. Then cells were incubated with the proper Alexa Fluor 488 anti-rabbit and 568 anti-mouse secondary antibodies (1 : 1000; Life Technologies) in 5% FBS in PBS and counter-stained with 300 nM DAPI for 3 min. Cells were mounted with ProLong Gold Antifade mountant (Life Technologies) and imaged using a laser-scanning confocal microscope (TCS SP5, Leica, Wetzlar, Germany) through a 63×/1.40 NA oil-immersion objective (HCX PL APO lambda blue). Z-stacks with 0.2 μm step size were acquired with sequential excitation at 1024 × 1024 pixels resolution and 1× or 2× magnification, 2 frames average. All image processing and analysis was performed using ImageJ software.

Mitochondrial network morphology

For the analysis of mitochondrial network morphology, z-stacks of cells labeled with COX5B antibody were used. Seven fovs randomly taken from at least three independent biological replicates were processed using a custom-written ImageJ macro (Appendix S1), consisting of several consecutive steps. A panel of spatial and shape description parameters (i.e., perimeter, area, circularity, roundness, solidity, and aspect ratio) among all z-planes was evaluated using the *Analyze Particles* function (Nikolaisen *et al.* 2014). In detail, circularity is defined as $4\pi \times \text{area}/(\text{perimeter})^2$ and it takes into account the compactness of the particles. The roundness, defined as $4 \times \text{area}/\pi \times (\text{major axis})^2$, is a measure of the particle shape relative to a perfect circle. Solidity represents the overall concavity of a particle and is defined as the area of the particle divided by the area of the convex hull of the particle: area/(convex area). The distribution density of all parameters was calculated for each fov and compared to the distribution density of all controls (i.e., particles from seven fovs) by the non-parametric Kolmogorov–Smirnov test to determine the distance between the empirical distribution functions of the samples. Significant ($p < 10^{-3}$) distances were analyzed by the non-parametric Kruskal–Wallis test followed by the post hoc Dunn's test for multiple comparisons. All data analysis and statistics procedures were written using the R environment for statistical computing (http://www.r-project.org/).

Three-dimensional reconstructions of mitochondrial networks were obtained from processed z-stacks using 3D Viewer ImageJ plug-in.

Immunofluorescence quantification and co-localization analysis

The rate of the mitophagic process was quantified as a decrease in mitochondrial content inside cells. Projections of z-stacks of COX5B and β-tubulin labeled cells were performed by summing all z-planes. To define cell area, a binary mask was created from β-tubulin signal and mitochondrial content was quantified as the COX5B intensity with respect to the β-tubulin area. At least four z-stacks obtained from three independent experiments were evaluated for each condition. To quantify the amount of PINK1 and parkin localized at the mitochondrial level, mitochondrial surface was measured on the four most representative planes of COX5B z-stack signals. After an automated thresholding process (*IsoData* function), the mitochondrial area was selected and transposed on PINK1 and parkin corresponding planes. Signals of PINK1 and parkin antibodies inside selected areas were measured and normalized with respect to mitochondrial area values. Co-localization analysis between COX5B and parkin signals was performed among all z-stacks with the *JaCoP* plugin (Bolte and Cordelières 2006), after transformation into 8-bit format. The degree of co-localization between two fluorescent labels was evaluated by the Manders' Overlap Coefficient, corresponding to the proportion of parkin signal overlapping to COX5B signal (Manders *et al.* 1992). At least four z-stacks were evaluated for each condition. Data are represented as mean ± SEM. Statistical analysis was performed with the Student's paired *t*-test with Welch correction for heteroscedasticity.

Results

Dopamine induces a significant dissipation of the mitochondrial membrane potential ($\Delta\psi_m$) and a fragmentation of the mitochondrial network

To determine the effect of dopamine on mitochondrial function, living cells were stained with Mitotracker Red CMXRos, which accumulates in mitochondria with an intact membrane potential. Treatment of SH-SY5Y cells with 250 μM dopamine for 6 and 24 h induced a significant loss of mitochondrial membrane potential. The same depolarization was achieved using the uncoupler CCCP (Fig. 1). Noticeably, both dopamine and CCCP treatments showed a 30–40% reduction in cell viability (Figure S1). Furthermore, dopamine strongly affected the mitochondrial network structure (Fig. 2a and b). Control cells showed a filamentous mitochondrial network with mitochondria distributed all over the soma, even along the dendrite-like processes, whereas dopamine-treated cells presented a disrupted mitochondrial network with mitochondria arranged in globular aggregates. Furthermore, the network perturbation induced by dopamine seemed to be strongly different from mitochondrial network alteration induced by CCCP treatment. To determine the quantitative and statistical relevance of these qualitative differences, our efforts were focused on finding shape description parameters that better reflected these morphological alterations. Among all parameters analyzed, the distribution density of circularity, roundness and solidity were better for highlighting morphological differences (Fig. 2c, d and e). When independent fovs were taken into account, the distribution density of circularity was observed to be significantly more distant from respective controls in CCCP-treated samples than in dopamine-treated samples.

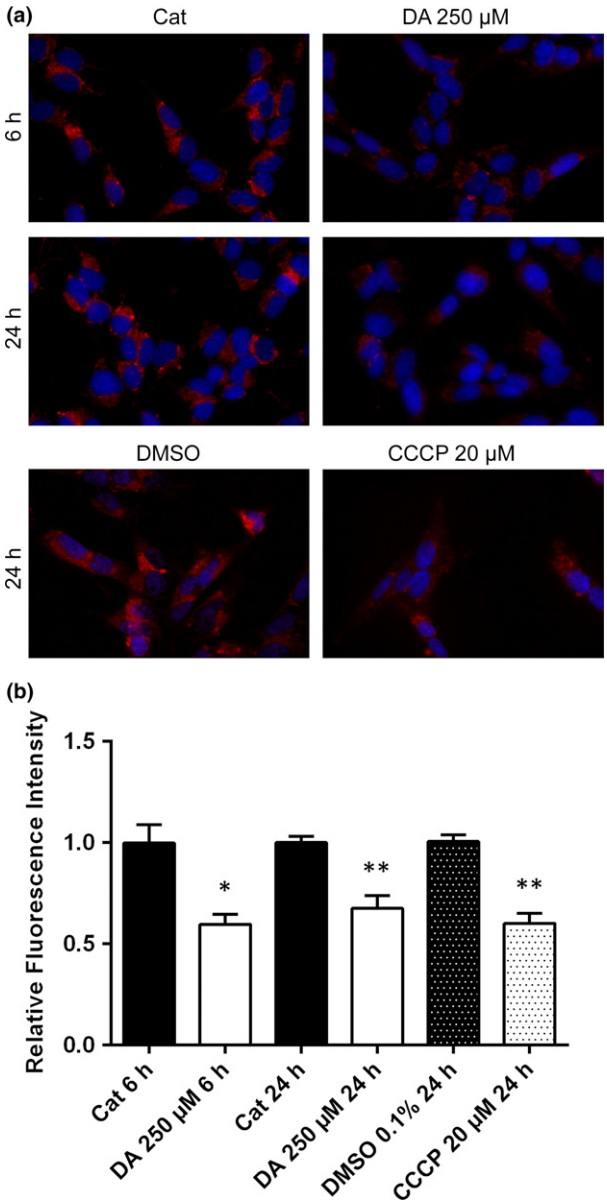

Fig. 1 Dopamine induces dissipation of mitochondrial potential. (a) Representative images of SH-SY5Y cells treated with 250 μM dopamine (DA 250 μM) in the presence of catalase, or treated with 20 μM carbonyl cyanide m-chlorophenylhydrazone (CCCP 20 μM) for 24 h. Red (Mitotracker) indicates mitochondria with intact $\Delta\Psi_m$. (b) Relative quantification of Mitotracker fluorescence normalized to nuclei emission (see text). Error bars represent SEM of four experiments.*$p < 0.05$; **$p < 0.01$.

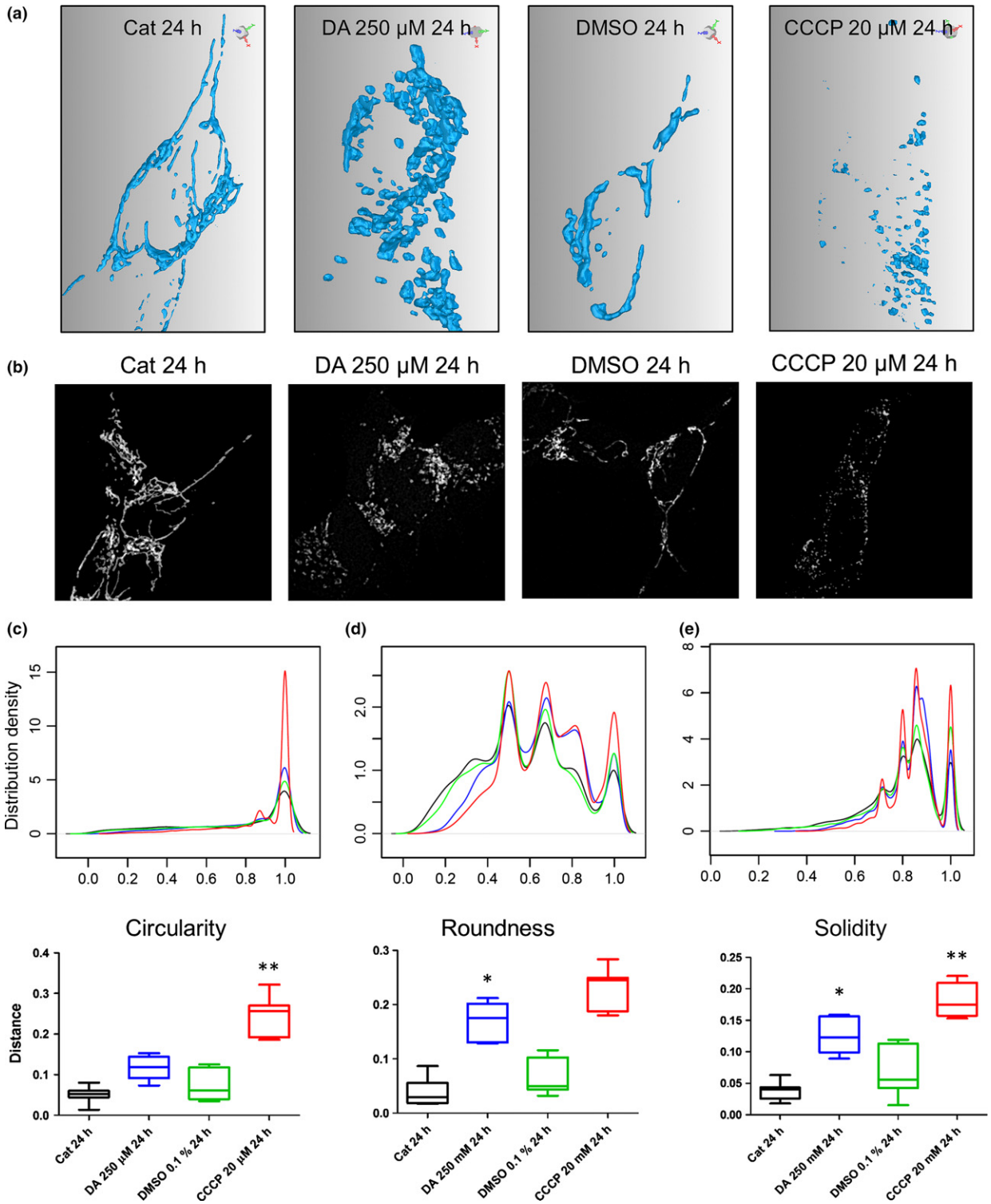

Fig. 2 Analysis of the mitochondrial network morphology. (a) Three-dimensional reconstructions of mitochondrial network from z-stacks with 0.2 µm step size. (b) Representative images of mitochondrial network obtained by automated image processing. (c, d, e) Distribution density (for all particles analyzed in seven fovs from at least three independent experiments) and Kolmogorov–Smirnov significant ($p < 10^{-3}$) distances (for any of the seven independent fovs) of circularity (c), roundness (d), and solidity (e) in the four experimental conditions. Black: catalase; blue: dopamine; green: dimethylsulfoxide (DMSO); red: carbonyl cyanide m-chlorophenylhydrazone (CCCP). Asterisks indicate significant differences in the medians in pairwise comparisons DA versus Cat and CCCP versus DMSO. *$p < 0.05$; **$p < 0.01$.

On the other hand, the distribution density of roundness and solidity was significantly affected by the dopamine treatment, though differently from the CCCP treatment.

Molecular characterization of mitochondrial network alterations

To characterize molecular differences inducing different mitochondrial network alterations, we analyzed abundance and modifications of OPA1 and MFN1 in our experimental conditions (Fig. 3). After dopamine treatment, we observed lower OPA1 levels (both the long OPA1-L and the short OPA1-S forms; Fig. 3a). CCCP induced the disappearance of OPA-L and increased levels of the OPA-S cleaved form.

On the other hand, we did not observe any effect on MFN1 levels or ubiquitination after dopamine treatment (Fig. 3b), whereas CCCP treatment induced a general down-regulation of MFN1, consequent to its ubiquitination (forms at a higher molecular weight).

Dopamine does not induce mitophagy

Both the quantification of immunofluorescence and western blot signal of COX5B, a protein localized in the mitochondrial inner membrane, did not suggest any significant variation in mitochondrial content inside cells after 24 h dopamine treatment, although mitochondria were depolarized; conversely, CCCP treatment induced a significant reduction in mitochondria (Fig. 4).

Dopamine does not induce an accumulation of PINK1 in mitochondria

To investigate how impaired dopamine homeostasis could interfere with quality control machinery, we performed a time-course evaluation of PINK1 protein level by Western blot analysis after 6 and 24 h dopamine treatment. As a reference positive control, we used a 20 μM CCCP treatment for 24 h. Dopamine did not induce an increase in full-length (64 kDa) PINK1 level neither in mitochondria-enriched fractions nor in whole-cells lysates at any time point, whereas full-length PINK1 protein level significantly rose after CCCP treatments (Fig. 5a and b). Western blot analysis was further confirmed by immunofluorescence quantification of PINK1 signal within the mitochondrial area (Fig. 5c and d).

Effect of dopamine on parkin mitochondrial localization

We verified parkin mitochondrial recruitment by immunofluorescence. We did not observe any significant increase in parkin at mitochondrial level after dopamine treatment, as shown in Fig. 6(a) and quantified in Fig. 6(b). In addition, to assess if dopamine could change the subcellular localization of parkin, we performed a co-localization analysis between parkin and COX5B in terms of Manders' Overlap Coefficient. Manders coefficient did not significantly change after dopamine exposure, whereas CCCP induced a significant increase in parkin fraction localized to mitochondria (Fig. 6c).

Dopamine also induced a small reduction in parkin total level (Fig. 6d and e). On the other hand, parkin total levels were sensibly reduced after CCCP treatment. It should be taken into account, however, that a parallel reduction was observed in the number of mitochondria (Fig. 4c). The Western blot pattern revealed the presence of a lower molecular weight band that did not show any significant correlation with the treatments.

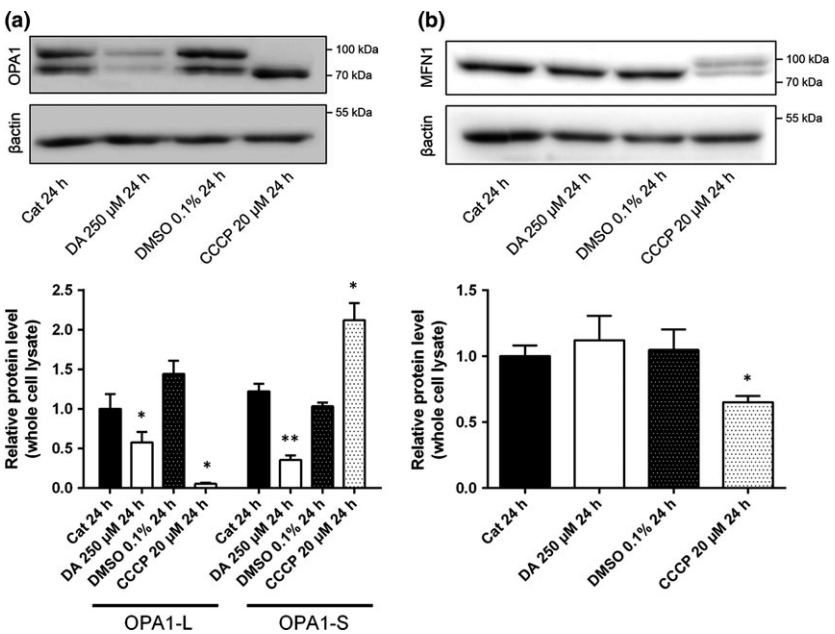

Fig. 3 Effect of dopamine on OPA1 and MFN1. (a) Representative Western blot image and related quantification of OPA1. Two forms are visible, the longest form (OPA1-L) and the shortest (OPA1-S). (b) Representative Western blot image and related quantification of MFN1. Bars represent the mean of three independent experiments of SH-SY5Y cells treated with 250 μM dopamine (DA 250 μM) in the presence of catalase, or treated with 20 μM carbonyl cyanide m-chlorophenylhydrazone (CCCP 20 μM) for 24 h. Error bars represent SEM of three experiments. *$p < 0.05$; **$p < 0.01$.

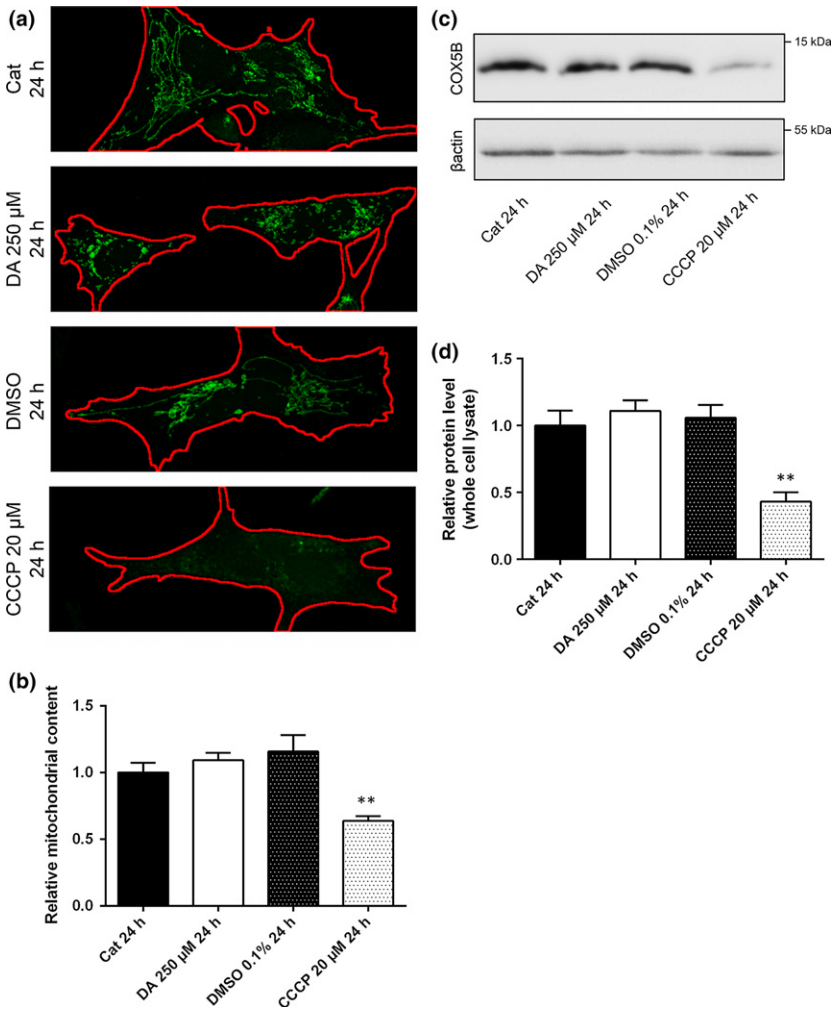

Fig. 4 Dopamine toxicity does not induce mitophagy. (a) Definition of the cell area (red) based on β-tubulin immunofluorescence. Mitochondria are represented in green (cytochrome c oxidase subunit 5B, COX5B signal). (b) Quantification of the mitochondria content per cell surface unit. The average of each control group was set to unit for normalization purposes. (c) A representative Western blot of COX5B. (d) Quantification of mitochondrial content (COX5B signal) with respect to total protein load (β-actin signal). Error bars represent SEM of four experiments. $^{**}p < 0.01$.

Effect of simultaneous treatment with dopamine and CCCP

We considered the effect of simultaneous treatment with dopamine and CCCP. As shown in Fig. 7(a), the co-treatment induced a remarkable depolarization of mitochondria in surviving cells, which are considerably reduced by the high toxicity of combined conditions. Similar to what was observed after CCCP-induced depolarization, PINK1 levels were raised (Fig. 7b). The number of mitochondria was lowered by the co-treatment to a greater extent as compared to the single CCCP treatment, and a similar behavior was observed for MFN1 levels. Moreover, the co-treatment affected the OPA1 processing as a sum of the two effects as taken standalone. Indeed, we observed both disappearance of OPA1-L, as induced by CCCP, and decrease in OPA1-S as after dopamine treatment. The co-treatment also increased the parkin localization to mitochondria (Fig. 7c). Worthy of note, different mitochondrial network morphologies were observed, from cells with a few residual mitochondria to cells with aggregated ones.

Discussion

In the last few years, several reports contributed to understand the role of PINK1 and parkin in the disposal of depolarized mitochondria (see Scarffe *et al.* 2014; Koyano and Matsuda 2015; Pickrell and Youle 2015). Briefly, a loss of $\Delta\Psi_m$ is thought to be sufficient to induce PINK1 accumulation in the OMM, PINK1-induced phosphorylation of ubiquitin and parkin, and parkin-mediated ubiquitination of OMM proteins (including VDAC1, mitofusins, and BNIP3L/NIX) (Geisler *et al.* 2010; Glauser *et al.* 2011; Kane *et al.* 2014; Gao *et al.* 2015). Controversial results indicate distinct parkin targets, suggesting that the mechanism of mitophagy induction is not unique and may be regulated by several factors, such as the cellular model being tested, the level of PINK1 and parkin, the toxin used to induce mitochondrial dysfunction, the time of exposure, and the inhibition of apoptosis and/or UPS proteolysis (Grenier *et al.* 2013). Here, we investigated the effects of the accumulation of cytosolic dopamine in SH-SY5Y cells

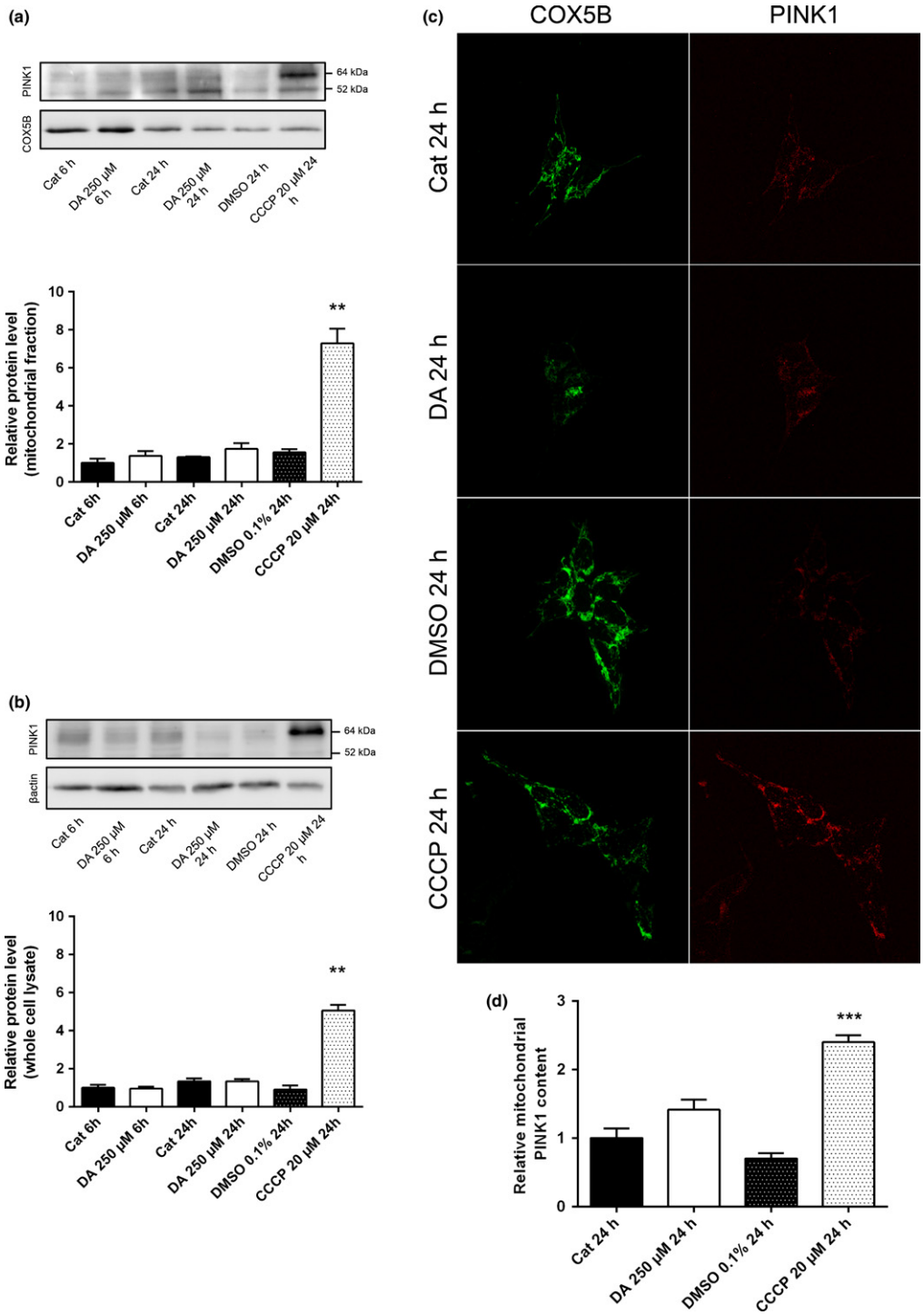

Fig. 5 Effect of dopamine on PINK1 protein level. (a) Protein quantification of the full-length (64 kDa) PINK1 by Western blot in mitochondria-enriched fractions. Cytochrome c oxidase subunit 5B (COX5B) was used for normalization. Carbonyl cyanide m-chlorophenylhydrazone (CCCP) treatment at 24 h represents the positive control. (b) Protein quantification of the full-length (64 kDa) PINK1 by Western blot in whole-cell lysates. CCCP treatment at 24 h represents the positive control. β-Actin was used for normalization. All values were normalized on the average value of the control group (Cat 6 h). (c) Representative images of COX5B (mitochondrial area) and PINK1 (quantification) signals. (d) Quantification of the PINK1 signal per mitochondrial surface unit. All values were normalized on the average value of the control group (Cat 24 h). Error bars represent SEM of four experiments. $^{**}p < 0.01$; $^{***}p < 0.0001$.

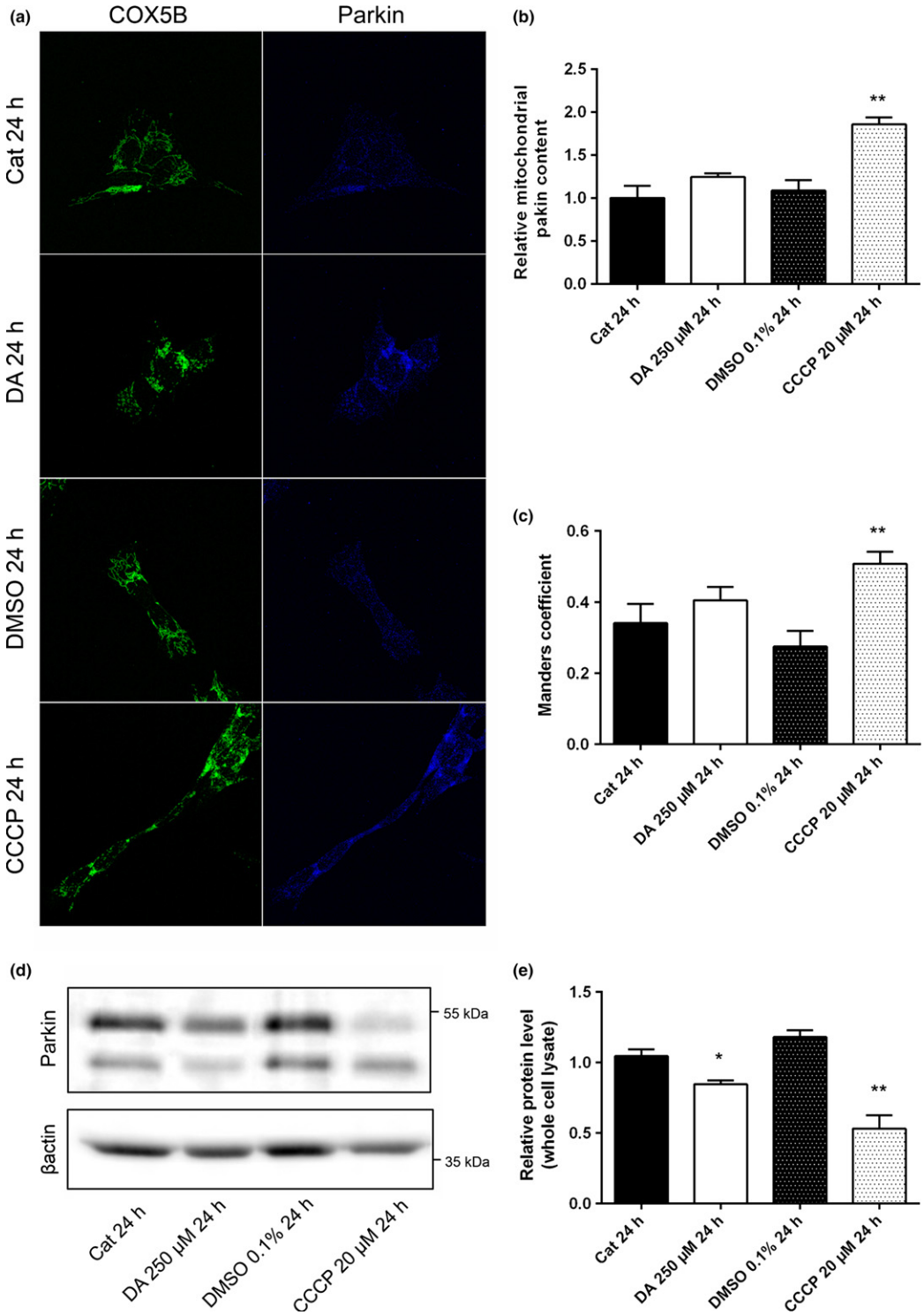

Fig. 6 Effect of dopamine on parkin mitochondrial localization. (a) Representative images of cytochrome c oxidase subunit 5B (COX5B) (mitochondrial area) and parkin (quantification) signals. (b) Quantification of the parkin signal per mitochondrial surface unit. All values were normalized on the average value of the control group (Cat 24 h). (c) Manders coefficient for the localization of parkin signal in COX5B-positive pixels. (d) Representative Western blot image of total parkin and (e) the related quantification. Error bars represent SEM of five experiments. $^{**}p < 0.01$.

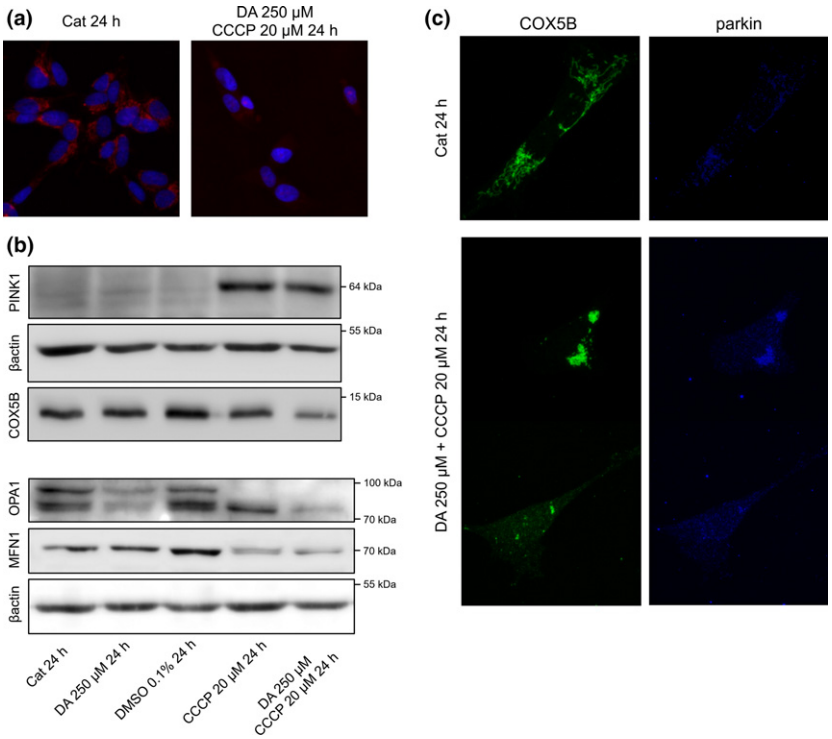

Fig. 7 Effect of the dopamine and carbonyl cyanide m-chlorophenylhydrazone (CCCP) co-treatment. (a) Simultaneous treatment with 250 µM dopamine and 20 µM CCCP-induced dissipation of the mitochondrial potential. Red (Mitotracker) indicates mitochondria with intact $\Delta\Psi_m$. (b) Representative western blot recapitulating dopamine and CCCP effects on PINK1, cytochrome c oxidase subunit 5B (COX5B), OPA1 and MFN1 levels and those of the co-treatment. (c) Representative immunofluorescence of the co-treatment, showing mitochondrial network morphology (COX5B) and parkin accumulation at the mitochondrial level.

(Alberio *et al.* 2014a). Despite being an undifferentiated cancer cell line, it possesses the genetic background to represent the ideal cell model to investigate PD pathogenesis (Krishna *et al.* 2014) and to study neurotoxicity in PD research (Cheung *et al.* 2009). Exposure to 250 µM dopamine in the presence of catalase displayed a moderate toxicity, similar to that of 20 µM CCCP. This concentration is able to increase intracellular ROS (Alberio *et al.* 2014a), whereas a lower concentration would yield an antioxidant effect (Alberio *et al.* 2010b).

We observed that dopamine toxicity acts in a way that differs with respect to the quality control mechanisms described above. Indeed, a marked $\Delta\Psi_m$ loss, comparable to that induced by the widely used uncoupler CCCP, was not followed by a proper disposal of depolarized mitochondria (mitophagy). Although the autophagy machinery is activated, as already described in the same conditions in a previous paper (Alberio *et al.* 2014a), the number of mitochondria is not lowered, as it is the case of CCCP treatment. Unlike many reports in the literature, we analyzed effects on the endogenous level of both PINK1 and parkin, thus avoiding their over-expression.

Also the mitochondrial network was perturbed differently by CCCP compared to dopamine. To substantiate this evidence further, we analyzed confocal microscopy images in terms of quantitative morphological descriptors (Nikolaisen *et al.* 2014). Among them, circularity, roundness and solidity displayed different distribution densities among controls (catalase and DMSO), dopamine and CCCP conditions, as quantified by the Kolmogorov–Smirnov test. Indeed, the organized network observed in our model under control conditions became disrupted and punctate by CCCP-induced depolarization, with values indicative of small, round, dispersed objects. On the other hand, dopamine led to more aggregated objects, with distribution densities of roundness and solidity that are significantly different from either control or CCCP conditions. It is noteworthy that circularity was not significantly affected by dopamine. We thus suppose that dopamine does not affect mitochondrial dynamics toward a high number of isolated mitochondria ready to be removed (fission); rather, it drives the network toward spheroidal mitochondrial aggregates (Otera *et al.* 2013).

The analysis of two regulators of mitochondrial dynamics, that is, OPA1 and MFN1, could explain the distinct alterations in the morphology of the mitochondrial network following dopamine and CCCP exposure (Kornmann 2014). As expected, CCCP led to complete removal of OPA1-L and enhancement of the lighter OPA1-S cleaved form. Although OPA1-S has been considered as a single band for quantitation purposes, it appeared evident that the cleaved form in CCCP-treated samples had a lower molecular weight. Actually, this form is the proteolytic formed by activated OMA1 (Anand *et al.* 2014), which inhibits IMM fusion in faulty mitochondria (Kornmann 2014). Conversely, dopamine induced a remarkable reduction in any OPA1 form, as already described after MPP^+ treatment (Ramonet *et al.* 2013). Interestingly, OPA1 down-regulation should also be

associated with the activation of the apoptosis intrinsic pathway (Ramonet *et al.* 2013). This could lead to a lack of fusion inhibition and mechanistically explain the peculiar morphology of the mitochondrial network in dopamine-treated cells. As a whole, dopamine perturbed the equilibrium between processes that regulate mitochondrial dynamics, possibly leading to the impairment of mitophagy.

Although alteration of dopamine homeostasis induced a remarkable $\Delta\Psi_m$ loss, comparable to that induced by CCCP, PINK1 full-length form (64 kDa) was not accumulated in the OMM, which is similar to what was observed after exposure to several complex I inhibitors including MPP^+ (Gao *et al.* 2015). Actually, dopamine alters the levels of several proteins that partially overlap with those changed after complex I inhibition by MPP^+ (Alberio *et al.* 2014b). Consequently, parkin could not be activated by PINK1 and did not localize to mitochondria. CCCP induced a remarkable recruitment of parkin to residual mitochondria and a parallel decrease in total parkin levels together with the total number of mitochondria. Conversely, dopamine treatment caused a small reduction in the total parkin level not correlated with mitochondria number. A truncated, functionally inactive parkin form (Muqit *et al.* 2004) was also observed at 40 kDa, without any significant change in its level. It appears therefore that the PINK1/parkin pathway was not properly activated, justifying also the lack of MFN1 ubiquitination by parkin and proper disposal (Gegg *et al.* 2010; Karbowski and Youle 2011). VDACs have been described as in charge of parkin recruitment to depolarized mitochondria (Sun *et al.* 2012). According to this view, the elimination of VDACs, induced by free cytosolic dopamine (Alberio *et al.* 2014a), should mechanistically explain the lack of parkin recruitment and mitophagy in our conditions.

As the depolarization induced by dopamine activates a different response with respect to that activated by CCCP, it is possible that molecular mechanisms triggered by a chemical uncoupler that dissipates the electrochemical potential of the IMM (i.e., CCCP) are different from those induced by the inhibition of the electron transport chain (i.e., MPP^+). Despite its pleiotropic action, dopamine may inhibit complex I and III (Van Laar *et al.* 2009; Jana *et al.* 2011) and its effects can be partially overlaid to those of complex I inhibitors. In addition, dopamine did not induce any effect on MFN1, a dynamin-related GTPase essential for OMM fusion, whereas CCCP-induced depolarization led to MFN1 degradation, as expected (Gegg *et al.* 2010). Therefore, mitochondrial depolarization alone is not a sufficient condition to inhibit protease(s) acting on PINK1, to recruit and activate parkin and to induce mitophagy. As PINK1 is constitutively degraded intra-mitochondrially (Jin and Youle 2012), it is possible that altered dopamine homeostasis does not affect the activity of proteases acting on PINK1. In turn, this lack of PINK1/parkin activation leads to incorrect disposal of depolarized mitochondria, which not only are functionally impaired but also generate further ROS and participate in apoptotic induction (Franco-Iborra *et al.* 2015).

It is interesting, however, that the simultaneous treatment with both CCCP and dopamine is able to trigger PINK1 accumulation, parkin recruitment and mitophagy. Nevertheless, this just confirms that the molecular machinery of the PINK1/parkin pathway can still be activated. It must be considered, however, that the double treatment has severe effects on cell viability and that any consideration is merely qualitative, as it is referred to a small population of survived cells. In addition, the mitochondrial network in these cells is quite heterogeneous, sometimes resembling the situation observed in the CCCP treatment alone (fragmented mitochondria) and sometimes resembling the situation of dopamine alone (aggregated mitochondria). Again, the analysis of the network is precluded by its heterogeneity and the small number of cells. Thus, the activation of the PINK1/pathway in neurons not yet degenerated should be possible, as PINK1 is still able to accumulate. The present body of results can be paralleled to pathogenetic mechanisms already described for sporadic Parkinson's disease (Pickrell and Youle 2015). Indeed, free cytosolic dopamine, which for several reasons originates from permeabilized synaptic vesicles (Lotharius and Brundin 2002; Segura-Aguilar *et al.* 2014), prevents the activation of the quality control program by impairing PINK1 accumulation in the OMM. In this way, failure of parkin recruitment to mitochondria resembles the loss of function of PINK1 in familial PARK6 patients. We hypothesize that oxidative stress, because of improper dopamine handling, was the major cause of the events we observed, even if we cannot exclude receptor-mediated effects.

In conclusion, the pleiotropic action of dopamine-induced cellular mechanisms leads first to mitochondrial depolarization, and then to the lack of PINK1 accumulation, alteration of the mitochondrial network (possibly led by OPA1 down-regulation) and accumulation of dysfunctional mitochondria. Mitophagy could be impaired in familiar PD linked to mutated PINK1, in which PINK1 lacks its ability to promote degradation of damaged mitochondria. Dopamine-induced toxicity could lead to a similar condition by inducing a mitochondrial dysfunction not followed by PINK1 activation of mitophagy, suggesting that defective renewal of mitochondria may be a leading event in sporadic PD.

Acknowledgments and conflict of interest disclosure

This work was partially supported by grant PRIN 2009CCZSES_003 from Ministero dell'Istruzione, dell'Università e della Ricerca of Italy to M.F. and by grant FAR2014 from University of Insubria to M.F., S.G., and T.A. Authors gratefully acknowledge Mr. Fabio Casolo Ginelli, Ms. Luisa Guidali, and Ms. Roberta Soroldoni for technical assistance. The authors have no conflict of interest to declare.

Supporting information

Additional supporting information may be found in the online version of this article at the publisher's web-site:

Figure S1. Effect of dopamine and CCCP on cell viability. Dopamine induced a moderate decrease in cell viability after 24 h. A similar reduction was observed after 24 h of 20 μM CCCP treatment. **p < 0.01; ***p < 0.005.

Appendix S1. Supplementary Methods.

References

Alberio T., Bossi A. M., Milli A., Parma E., Gariboldi M. B., Tosi G., Lopiano L. and Fasano M. (2010a) Proteomic analysis of dopamine and α-synuclein interplay in a cellular model of Parkinson's disease pathogenesis. *FEBS J.* **277**, 4909–4919.

Alberio T., Colapinto M., Natale M., Ravizza R., Gariboldi M. B., Bucci E. M., Lopiano L. and Fasano M. (2010b) Changes in the two-dimensional electrophoresis pattern of the Parkinson's disease related protein DJ-1 in human SH-SY5Y neuroblastoma cells after dopamine treatment. *IUBMB Life* **62**, 688–692.

Alberio T., Lopiano L. and Fasano M. (2012) Cellular models to investigate biochemical pathways in Parkinson's disease. *FEBS J.* **279**, 1146–1155.

Alberio T., Mammucari C., D'Agostino G., Rizzuto R. and Fasano M. (2014a) Altered dopamine homeostasis differentially affects mitochondrial voltage-dependent anion channels turnover. *Biochim. Biophys. Acta* **184**, 1816–1822.

Alberio T., Bondi H., Colombo F., Alloggio I., Pieroni L., Urbani A. and Fasano M. (2014b) Mitochondrial proteomics investigation of a cellular model of impaired dopamine homeostasis, an early step in Parkinson's disease pathogenesis. *Mol. BioSyst.* **10**, 1332–1344.

Anand R., Wai T., Baker M. J., Kladt N., Schauss A. C., Rugarli E. and Langer T. (2014) The i-AAA protease YME1L and OMA1 cleave OPA1 to balance mitochondrial fusion and fission. *J. Cell Biol.* **204**, 919–929.

Blum D., Torch S., Nissou M. F., Benabid A. L. and Verna J. M. (2000) Extracellular toxicity of 6-hydroxydopamine on PC12 cells. *Neurosci. Lett.* **283**, 193–196.

Bolte S. and Cordelières F. P. (2006) A guided tour into subcellular colocalization analysis in light microscopy. *J. Microsc.* **224**, 213–232.

Bonifati V. (2012) Autosomal recessive parkinsonism. *Parkinsonism Relat. Disord.* **18**(Suppl 1), S4–S6.

Caudle W. M., Colebrooke R. E., Emson P. C. and Miller G. W. (2008) Altered vesicular dopamine storage in Parkinson's disease: a premature demise. *Trends Neurosci.* **31**, 303–308.

Cheung Y. T., Lau W. K., Yu M. S., Lai C. S., Yeung S. C., So K. F. and Chang R. C. (2009) Effects of all-trans-retinoic acid on human SH-SY5Y neuroblastoma as in vitro model in neurotoxicity research. *Neurotoxicology* **30**, 127–135.

Franco-Iborra S., Vila M. and Perier C. (2015) The Parkinson disease mitochondrial hypothesis: where are we at? *Neuroscientist*. Epub ahead of print.

Frezza C., Cipolat S. and Scorrano L. (2007) Organelle isolation: functional mitochondria from mouse liver, muscle and cultured fibroblasts. *Nat. Protoc.* **2**, 287–295.

Gao F., Chen D., Si J., Hu Q., Qin Z., Fang M. and Wang G. (2015) The mitochondrial protein BNIP3L is the substrate of PARK2 and mediates mitophagy in PINK1/PARK2 pathway. *Hum. Mol. Genet.* **24**, 2528–2538.

Gegg M. E., Cooper J. M., Chau K. Y., Rojo M., Schapira A. H. and Taanman J. W. (2010) Mitofusin 1 and mitofusin 2 are ubiquitinated in a PINK1/parkin-dependent manner upon induction of mitophagy. *Hum. Mol. Genet.* **19**, 4861–4870.

Geisler S., Holmström K. M., Skujat D., Fiesel F. C., Rothfuss O. C., Kahle P. J. and Springer W. (2010) PINK1/Parkin-mediated mitophagy is dependent on VDAC1 and p62/SQSTM1. *Nat. Cell Biol.* **12**, 119–131.

Glauser L., Sonnay S., Stafa K. and Moore D. J. (2011) Parkin promotes the ubiquitination and degradation of the mitochondrial fusion factor mitofusin 1. *J. Neurochem.* **118**, 636–645.

Gómez-Santos C., Ferrer I., Santidrián A. F., Barrachina M., Gil J. and Ambrosio S. (2003) Dopamine induces autophagic cell death and alpha-synuclein increase in human neuroblastoma SH-SY5Y cells. *J Neurosci Res.* **73**, 341–350.

Grenier K., McLelland G. L. and Fon E. A. (2013) Parkin- and PINK1-Dependent Mitophagy in Neurons: will the Real Pathway Please Stand Up? *Front. Neurol.* **4**, 100.

Guillot T. S. and Miller G. W. (2009) Protective actions of the vesicular monoamine transporter 2 (VMAT2) in monoaminergic neurons. *Mol. Neurobiol.* **39**, 149–170.

Hauser D. N. and Hastings T. G. (2013) Mitochondrial dysfunction and oxidative stress in Parkinson's disease and monogenic parkinsonism. *Neurobiol. Dis.* **51**, 35–42.

Jana S., Sinha M., Chanda D., Roy T., Banerjee K., Munshi S., Patro B. S. and Chakrabarti S. (2011) Mitochondrial dysfunction mediated by quinone oxidation products of dopamine: implications in dopamine cytotoxicity and pathogenesis of Parkinson's disease. *Biochim. Biophys. Acta* **1812**, 663–673.

Jin S. M. and Youle R. J. (2012) PINK1- and Parkin-mediated mitophagy at a glance. *J. Cell Sci.* **125**, 795–799.

Jin S. M., Lazarou M., Wang C., Kane L. A., Narendra D. P. and Youle R. J. (2010) Mitochondrial membrane potential regulates PINK1 import and proteolytic destabilization by PARL. *J. Cell Biol.* **191**, 933–942.

Kane L. A., Lazarou M., Fogel A. I., Li Y., Yamano K., Sarraf S. A., Banerjee S. and Youle R. J. (2014) PINK1 phosphorylates ubiquitin to activate Parkin E3 ubiquitin ligase activity. *J. Cell Biol.* **205**, 143–153.

Karbowski M. and Youle R. J. (2011) Regulating mitochondrial outer membrane proteins by ubiquitination and proteasomal degradation. *Curr. Opin. Cell Biol.* **23**, 476–482.

Kornmann B. (2014) Quality control in mitochondria: use it, break it, fix it, trash it. *F1000Prime Rep.* **6**, 15.

Koyano F. and Matsuda N. (2015) Molecular mechanisms underlying PINK1 and parkin catalyzed ubiquitylation of substrates on damaged mitochondria. *Biochim. Biophys. Acta* **1853**, 2791–2796.

Krishna A., Biryukov M., Trefois C. *et al.* (2014) Systems genomics evaluation of the SH-SY5Y neuroblastoma cell line as a model for Parkinson's disease. *BMC Genom.* **15**, 1154.

Lotharius J. and Brundin P. (2002) Pathogenesis of Parkinson's disease: dopamine, vesicles and alpha-synuclein. *Nat. Rev. Neurosci.* **3**, 932–942.

Manders E. M., Stap J., Brakenhoff G. J., van Driel R. and Aten J. A. (1992) Dynamics of three-dimensional replication patterns during the S-phase, analysed by double labelling of DNA and confocal microscopy. *J. Cell Sci.* **103**, 857–862.

Matsuda N., Sato S., Shiba K. *et al.* (2010) PINK1 stabilized by mitochondrial depolarization recruits parkin to damaged mitochondria and activates latent parkin for mitophagy. *J. Cell Biol.* **189**, 211–221.

Mena M. A., de Yébenes J., Dwork A., Fahn S., Latov N., Herbert J., Flaster E. and Slonin D. (1989) Biochemical properties of monoamine-rich human neuroblastoma cells. *Brain Res.* **486**, 286–296.

Muqit M. M., Davidson S. M., Payne Smith M. D., MacCormac L. P., Kahns S., Jensen P. H., Wood N. W. and Latchman D. S. (2004)

Parkin is recruited into aggresomes in a stress-specific manner: over-expression of parkin reduces aggresome formation but can be dissociated from parkin's effect on neuronal survival. *Hum. Mol. Genet.* **13**, 117–135.

Narendra D. P. and Youle R. J. (2011) Targeting mitochondrial dysfunction: role for PINK1 and parkin in mitochondrial quality control. *Antioxid. Redox Signal.* **14**, 1929–1938.

Narendra D. P., Jin S. M., Tanaka A., Suen D. F., Gautier C. A., Shen J., Cookson M. R. and Youle R. J. (2010) PINK1 is selectively stabilized on impaired mitochondria to activate Parkin. *PLoS Biol.* **8**, e1000298.

Nikolaisen J., Nilsson L. I., Pettersen I. K., Willems P. H., Lorens J. B., Koopman W. J. and Tronstad K. J. (2014) Automated quantification and integrative analysis of 2D and 3D mitochondrial shape and network properties. *PLoS ONE* **9**, e101365.

Otera H., Ishihara N. and Mihara K. (2013) New insights into the function and regulation of mitochondrial fission. *Biochim. Biophys. Acta* **1833**, 1256–1268.

Pickrell A. M. and Youle R. J. (2015) The roles of PINK1, parkin, and mitochondrial fidelity in Parkinson's disease. *Neuron* **85**, 257–273.

Ramonet D., Perier C., Recasens A., Dehay B., Bové J., Costa V., Scorrano L. and Vila M. (2013) Optic atrophy 1 mediates mitochondria remodeling and dopaminergic neurodegeneration linked to complex I deficiency. *Cell Death Differ.* **20**, 77–85.

Scarffe L. A., Stevens D. A., Dawson V. L. and Dawson T. M. (2014) Parkin and PINK1: much more than mitophagy. *Trends Neurosci.* **37**, 315–324.

Segura-Aguilar J., Paris I., Muñoz P., Ferrari E., Zecca L. and Zucca F. A. (2014) Protective and toxic roles of dopamine in Parkinson's disease. *J. Neurochem.* **129**, 898–915.

Sun Y., Vashisht A. A., Tchieu J., Wohlschlegel J. A. and Dreier L. (2012) Voltage-dependent anion channels (VDACs) recruit Parkin to defective mitochondria to promote mitochondrial autophagy. *J. Biol. Chem.* **287**, 40652–40660.

Van Laar V. S., Mishizen A. J., Cascio M. and Hastings T. G. (2009) Proteomic identification of dopamine-conjugated proteins from isolated rat brain mitochondria and SH-SY5Y cells. *Neurobiol. Dis.* **34**, 487–500.

Youle R. J. and van der Bliek A. M. (2012) Mitochondrial fission, fusion, and stress. *Science* **337**, 1062–1065.